Investigation of seismicity after the initiation of a Seismic Electric Signal activity until the main shock

By N. V. Sarlis,[*1] E. S. Skordas,[*1] M. S. Lazaridou[*1] and P. A. Varotsos[*1,†]

(Communicated by Seiya Uyeda, M.J.A.)

Abstract: The behavior of seismicity in the area candidate to suffer a main shock is investigated after the observation of the Seismic Electric Signal activity until the impending main shock. This is based on the view that the occurrence of earthquakes is a critical phenomenon to which statistical dynamics may be applied. In the present work, analysing the time series of small earthquakes, the concept of natural time χ was used and the results revealed that the approach to criticality itself can be manifested by the probability density function (PDF) of κ_1 calculated over an appropriate statistical ensemble. Here, κ_1 is the variance $\kappa_1(=\langle\chi^2\rangle-\langle\chi\rangle^2)$ resulting from the power spectrum of a function defined as $\Phi(\omega)=\sum_{k=1}^{N} p_k \exp(i\omega\chi_k)$, where p_k is the normalized energy of the k-th small earthquake and ω the natural frequency. This PDF exhibits a maximum at $\kappa_1 \approx 0.070$ a few days before the main shock. Examples are presented, referring to the magnitude 6∼7 class earthquakes that occurred in Greece.

Keywords: Seismic Electric Signals, natural time, time-window

1. Introduction

Seismic Electric Signals (SES) are transient low frequency (≤ 1 Hz) electric signals that have been observed in Greece,[1)–7)] Japan,[8),9)] and Mexico[10)] months to days before earthquakes (EQs hereafter). They are considered as emitted when the stress in the focal region reaches a critical value before the failure.[11),12)] This is interpreted as stemming from the fact that a stress variation affects the Gibbs energy for the defect formation,[13)] migration[14)] and activation[15)] in solids and that the electric dipoles formed by defects exhibit a cooperative orientation when the stress reaches a critical value. EQs exhibit complex correlations in space, time and magnitude (M (Athens Obs.), Mw (USGS), hereafter) as shown by many studies, e.g.,[16)–23)] in agreement with the repeatedly proposed view that EQs occur also at a critical point (e.g., Ref. 24) see also Ref. 25) and references therein). The view that both SES emission and EQ occurrence are critical phenomenon and that the approach to "electrical" critical point shortly precedes the approach to "mechanical" critical point is our fundamental premise for short-term EQ prediction.

During the past decade, a method of time series analysis for identifying the approach of a dynamic process to a critical state has been developed, based on the concept of a new time frame, named natural time.[12),26)–28)] The principle of the natural time analysis is as follows.

In a time series consisting of N events, the natural time $\chi_k = k/N$ serves as an index for the occurrence of the k-th event. The evolution of the pair (χ_k, Q_k) is studied, where Q_k denotes a quantity proportional to the energy released in the k-th event. For dichotomous signals, which is frequently the case of SES activities (a sequence of SES observed within a short time (e.g., ≈ hours) is termed SES activity), Q_k can be replaced by the duration of the k-th pulse. In the case of seismicity, Q_k may be taken as the seismic moment M_{0k} of the k-th event, since M_0 is roughly proportional to the energy released during an EQ. Then, we calculate the normalized power spectrum $\Pi(\omega) \equiv |\Phi(\omega)|^2$, where

$$\Phi(\omega)=\sum_{k=1}^{N} p_k \exp\left(i\omega\frac{k}{N}\right)=\sum_{k=1}^{N} p_k \exp(i\omega\chi_k) \quad [1]$$

[*1] Solid State Section and Solid Earth Physics Institute, Physics Department, University of Athens, Athens, Greece.
[†] Correspondence should be addressed: P.A. Varotsos, Solid State Section and Solid Earth Physics Institute, Physics Department, University of Athens, Panepistimiopolis, Zografos 157 84, Athens, Greece (e-mail: pvaro@otenet.gr).

doi: 10.2183/pjab/84.331

In Eq. [1], p_k is the normalized energy of k-th event $p_k = Q_k / \sum_{n=1}^{N} Q_n$ and $\omega = 2\pi\phi$, where ϕ denotes the natural frequency. In Eq. [1], $\Phi(\omega)$ is a continuous function which should not be confused with the usual discrete Fourier transform, because the latter considers only the relevant values at $\phi = 0, 1, 2, \ldots$. In natural time analysis, the properties of $\Pi(\omega)$ or $\Pi(\phi)$ are studied for continuous natural frequency ϕ less than 0.5. This is so, because in this range of ϕ, $\Pi(\omega)$ or $\Pi(\phi)$ reduces to a characteristic function for the probability distribution p_k in the context of probability theory (see p. 499 of Ref. 29)). This means that statistical properties, such as variance, can be obtained by its derivatives at the origin, i.e., $\omega \to 0$.

It has been shown theoretically that the following relation holds when the system enters the critical stage (see pp. 259–260 of Ref. 12), Ref. 26), Appendix A and B of Ref. 28))

$$\Pi(\omega) = \frac{18}{5\omega^2} - \frac{6\cos\omega}{5\omega^2} - \frac{12\sin\omega}{5\omega^3} \qquad [2]$$

which for $\omega \to 0$, simplifies to

$$\Pi(\omega) \approx 1 - 0.07\omega^2.$$

This relation shows that the second order Taylor expansion coefficient of $\Pi(\omega)$, labelled κ_1 is 0.070. The quantity κ_1 equals to the variance $\langle\chi^2\rangle - \langle\chi\rangle^2$ of natural time χ, i.e.,

$$\kappa_1 = \langle\chi^2\rangle - \langle\chi\rangle^2 = 0.070 \qquad [3]$$

where $\langle f(\chi)\rangle = \sum_{k=1}^{N} p_k f(\chi_k)$. Furthermore, it was observed for several EQs that κ_1 slowly approaches to 0.070 just before the main shocks and abruptly changed to vanishingly small when the main shocks occurred. On this basis, it was proposed that κ_1 (or $\Pi(\omega)$ for $\omega \to 0$) may be considered as an order parameter for seismicity.[28)]

In addition to κ_1 (or $\Pi(\omega)$ for $\omega \to 0$), another quantity useful from statistical dynamics point of view was introduced.[12),26),30)] It is the entropy S defined as

$$S \equiv \langle\chi \ln\chi\rangle - \langle\chi\rangle \ln\langle\chi\rangle.$$

This quantity satisfies the conditions for a function to be defined as entropy, namely the positivity and concavity as well as stability or experimental robustness.[31)] It differs from the usual entropy since it depends on the sequential order of events[32)] so that its value changes to a different one, labelled S_-, upon considering the time reversal.[31),33)] The S value for a "uniform" distribution of Q_k, e.g., when all p_k are equal, is $\ln(2)/2 - (1/4) \approx 0.0966$ which is designated S_u. The SES activities, when analyzed in natural time, have been found to obey the following conditions:[33),34)]

$$S, S_- < S_u \qquad [4]$$

In the investigation of seismicity, the behaviour of κ_1, the order parameter of seismicity[28)] during the period after the SES activity until the main shock in the area candidate to suffer a strong EQ is studied. It has been shown that this study enabled the shortening of the time-window of the prediction of impending main shock to the range of a few days to a few hours.[12),26),33)–35)] But there has been some room for subjective judgement to identify the approach to critical stage because the time variations of parameters were traced on only a single time series (χ_k, Q_k). Introduction of an important improvement of the procedure constitutes the basic aim of the present paper. The new procedure is supposed to be more objective since the approach to criticality is recognized by changes in probability density functions as will be explained in Section 2. As examples, we apply this procedure in Section 3 to the most recent SES and seismicity data in Greece.

2. The new method using natural time for shortening the time-window of short-term EQ prediction

2.1 The approach employed in our previous studies. Natural time analysis reveals, as mentioned in Section 1, that $\Pi(\omega)$ for $\omega \to 0$ or κ_1 can be considered as an order parameter for seismicity. To obtain $\Pi(\omega)$ for $\omega \to 0$ or κ_1, however, it is necessary to decide the initiation time of seismicity analysis. We decided to start the analysis immediately after the SES initiation. This is based on our fundamental premise, stated in Section 1, that both SES emission and EQ occurrence are critical phenomenon and the approach to "electrical" critical point shortly precedes "mechanical" critical point.

Once a SES activity has been recorded, the area to suffer the main shock can be estimated on the basis of the so-called selectivity map[4),12),36)–38)] of the station at which the SES was recorded. Thus, we have some area, hereafter labelled A, in

which we count the small EQs, e_i, that occur after the initiation of the SES activity. Each EQ e_i is characterized by its epicentral location $\mathbf{x}(e_i)$, the conventional time of its occurrence $t(e_i)$, and its magnitude $M(e_i)$ or the equivalent seismic moment $M_0(e_i)$. The index $i = 1, 2, \ldots$, increases by one each time a new EQ with M larger or equal to some threshold M_{thres} occurs within the area A. Thus, a set of events A, denoted as $A_{Mthres} = \{e_i \in A : M(e_i) \geq M_{thres}\}$, is formed each time until the main shock occurs in A at $i = N$. Therefore, a family of N! sets of A_{Mthres} should have been formed at the main shock. Here, the number of EQs in A_{Mthres} is denoted by $|A_{Mthres}|$. Since, in forming A_{Mthres}, we place the EQs in the sequence of their occurrence time, A_{Mthres} is a time ordered set.

It has been repeatedly confirmed that, for at least one magnitude threshold M_{thres} the conditions [3] and [4], i.e., $\kappa_1(A_{Mthres}) \approx 0.070$ and $S(A_{Mthres})$ and $S_-(A_{Mthres}) < S_u$, were satisfied by the small EQs in the area A a few days to a few hours before the main shock.[12),26),33)–35)] Thus, such a study enables, in principle, prediction of the main shock to be made within a few days to a few hours before its occurrence.

The actual procedure was carried out as follows: We set the natural time zero at the initiation time of the SES activity, and then formed time series of seismic events in natural time for the area A each time when a small EQ ($M \geq M_{thres}$) occurred, in other words when the number of the events increased by one. The normalized power spectrum in natural time $\Pi(\phi)$ for each of the time series was computed for the pairs (χ_k, Q_k) and compared with that of Eq. [2] for $\phi \in [0, 0.5]$. We also calculated the evolution of the quantities κ_1, S and S_- to ascertain Eq. [4] was also satisfied. The actual criteria for recognizing a true coincidence of the observed time series with that of critical state were as follows:[12),26),33)–35)] First, the 'average' distance $\langle D \rangle$ between the curves of $\Pi(\phi)$ of the evolving seismicity and Eq. [2] should be smaller than 10^{-2}. This was a practical criterion for stopping calculation. Second, the final approach of κ_1 of the evolving $\Pi(\phi)$ to that of Eq. [2], i.e., 0.070, must be by descending from above. This rule was found empirically.[26)] Third, both values S and S_- should be smaller than S_u at the coincidence. Finally and fourth, since the process concerned is supposed to be self-similar (critical dynamics), the time of the occurrence of the true coincidence should not vary, in principle, upon changing (within reasonable limits) the size of area A and the magnitude threshold M_{thres}. Although the method worked, it was felt that the criteria were somewhat subjective.

2.2 New approach suggested here upon using P_{Mthres} or the $\varepsilon[A_{Mthres}]$ ensemble. The basic idea behind the new approach suggested in this paper is the following: When area A reaches criticality, one expects in general that all its subareas have also reached criticality simultaneously. At that time, therefore, each of these subareas would be expected to give subsets with certain values of κ_1 close to 0.070, but perhaps with a statistical probability centered at 0.070, assuming equi-partition of probability among these subsets. Before the criticality is reached, κ_1-values will not show such a distribution.

In practice, in order to check whether criticality as described above has been approached at the occurrence of a new event i within the predicted area A, we should construct all the possible proper subsets of A_{Mthres} that *necessarily* include the event i and examine if their κ_1-values reveal the probability distribution centered at 0.070. A subset is qualified as a proper subset (P_{Mthres}) if and only if it includes all EQs that took place inside its corresponding rectangular subarea, i.e., $R(P_{Mthres})$. This is, of course, a simplification-followed throughout the present paper- because other geometries, e.g., circular, could be also considered.

Let us now consider an example shown in Fig. 1, in which four EQs have occurred (A is indicated by a black line rectangle in each panel) in a sequence indicated by the numbers i = 1, 2, 3 and 4. Colored rectangles depict proper subareas $R(P_{Mthres}) = R_j(i)$ just after the occurrence of each EQ. Figure 1 shows that the number of subareas j increases by an integer larger than or equal to one, when one EQ e_i occurs. For each of these proper subsets (which form the $\varepsilon[A_{Mthres}]$ ensemble at each time instant), one can compute the κ_1 values and then construct their distribution denoted $Prob(\kappa_1)$ hereafter. Just after the occurrence of the second event a single proper subset can be defined, thus only $\kappa_1[R_1(2)]$ is available. Just after the occurrence of the third event, three proper subsets of A_{Mthres} can be defined as shown in Fig. 1. Recall that the

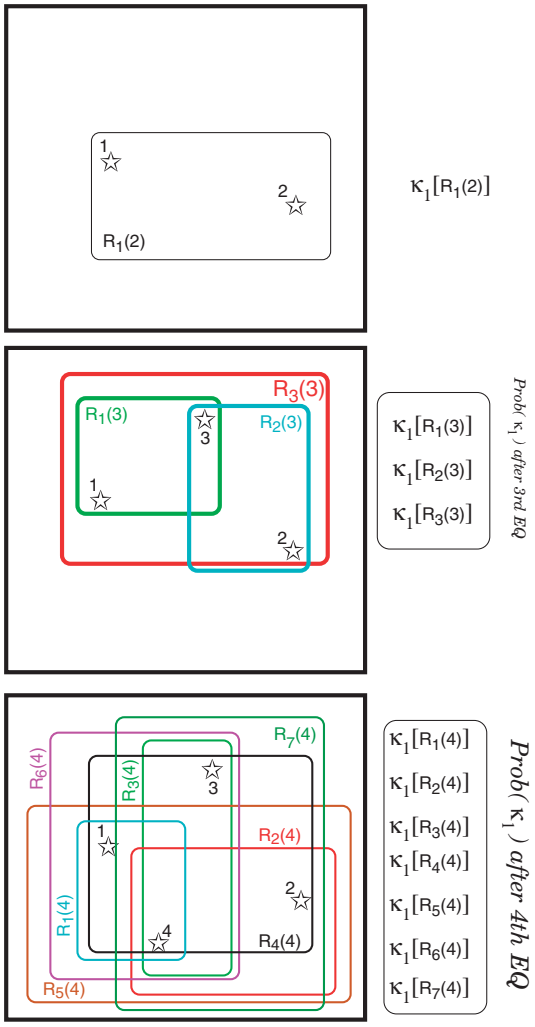

Fig. 1. The area A (in thick black rectangle) and its rectangular subareas $R_j(i)$, corresponding to the proper subsets immediately after the occurrence of the second EQ "2" (upper panel), the third EQ "3" (middle panel) and the fourth EQ "4" (bottom panel). The location of each EQ is shown by an open star. Right column shows that κ_1 values can be obtained for each subset.

necessary condition for a proper subset at a given time instant is that it includes the last event (the third EQ in this case). Therefore, $\kappa_1[R_1(2)]$ obtained before the third event is not included for the construction of the distribution Prob(κ_1) at the instant of the third event. By the same token, after the occurrence of the fourth event, seven proper subsets result. Thus, we can now calculate κ_1 for each of these 7 subsets and construct the Prob(κ_1) versus κ_1 graph to examine whether it maximizes at $\kappa_1 \approx 0.070$ (i.e., if it obeys Eq. [3]). In actual cases, number of EQs, depending on the threshold magnitude, are usually many tens and the number of subareas a few to several thousands. Then by performing an averaging procedure over *all* those proper subsets we expect that the average will also satisfy Eq. [3].

In the new approach, the κ_1-values of all these subareas and the largest area A, are treated on *equal* footing, which means that the adopted largest area A may be a proper subarea of a larger area in which the main shock actually occurs. This is a useful notion when the selectivity map of the concerned station is incomplete or a portion of it is adopted for some reason as in the case of Subsection 3.5.

We shall demonstrate in the next section, by applying the new procedure to the cases of the most recent SES activities and associated EQs in Greece, that it seems to help determining the time-window of the impending main shock with much less arbitrariness than the previous method.

3. The application of the proposed procedure to the most recent examples

In the following, we will describe the case studies for the recent Greek events. In Fig. 2, we depict four SES activities that have been recently recorded at the stations PAT (in central Greece) and PIR (western Greece):

Fig. 2(a) on Nov. 7, 2007, at PAT
Fig. 2(b) on Jan. 10, 2008, at PAT
Fig. 2(c) on Jan. 14, 2008, at PIR
Fig. 2(d) on Feb. 9, 2008, at PAT.

In addition, we illustrate, in Fig. 3, long duration (lasting for several days) SES activities recorded recently at PIR.

Fig. 3(a) from Jan. 21 to 26, 2008
Fig. 3(b) from Feb. 29 to March 2, 2008

These have been ascertained to be SES activities by applying the usual criteria (i.e., the conditions [3] and [4]) as explained in Refs. 39)–41). We now apply the present procedure to all these cases. Here, we present the results for the magnitude threshold $M_{thres} = 3.2$, but additional thresholds ($M_{thres} = 3.1$ and 3.3) were also checked to ensure magnitude threshold invariance of the results (cf. In one case, discussed in Subsection 3.5, higher magnitude thresholds have been considered for the reasons that will be explained there).

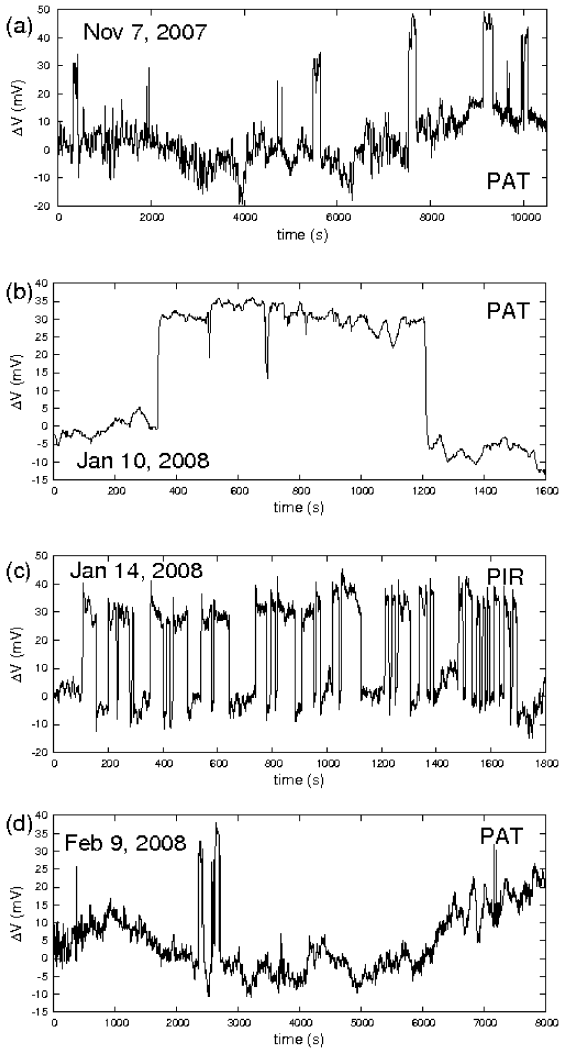

Fig. 2. Recent SES activities recorded in Greece.

3.1 The case of the SES activity at PAT on Nov. 7, 2007. The investigation of the seismicity subsequent to that SES activity (Fig. 2(a)) was made[39] in the area A: $N_{37.6}^{38.6}E_{20.0}^{23.3}$ inferred from the selectivity of PAT. At 05:14 UT on Jan. 6, 2008, a major EQ (M6.6) occurred with epicenter at 37.1°N 22.8°E, i.e., about 50 km to the south of the area A. What happened before that EQ can be seen in Fig. 4 ($M_{thres} = 3.2$), which shows that Prob(κ_1) maximizes at around $\kappa_1 = 0.073$ upon the occurrence of a small event at 04:49 on Jan. 4, 2008, i.e., almost two days before the main shock. In this case, it was found $\langle \kappa_1(P_{Mthres}) \rangle_{\varepsilon[A_{Mthres}]} = 0.070$ with standard deviation 0.008. (The symbol $\langle \kappa_1(P_{Mthres}) \rangle_{\varepsilon[A_{Mthres}]}$ stands for the average value obtained when using the ensemble $\varepsilon[A_{Mthres}]$).

3.2 The case of the SES activity at PAT on Jan. 10, 2008. For this SES activity (Fig. 2(b)), the investigation of the seismicity was also made in the area A: $N_{37.6}^{38.6}E_{20.0}^{23.3}$.[40] The results are shown in Fig. 5 ($M_{thres} = 3.2$), where we see that Prob(κ_1) exhibits a bimodal feature. A secondary peak at $\kappa_1 \approx 0.070$ (not exactly 0.070 but close) tends to become gradually dominant on around Jan. 31. Actually, at 20:25 UT and 22:15 UT on Feb. 4, 2008, two EQs with magnitudes 5.4 and 5.5 occurred at around 38.1°N 21.9°E inside the studied area A at a small distance (≈10 km) from the measuring station PAT.

The bimodal feature in Fig. 5 might, in some way, be related to the occurrence of the two EQs with comparable magnitudes, i.e., M ≈ 5.5, but its mechanism is unknown at this stage.

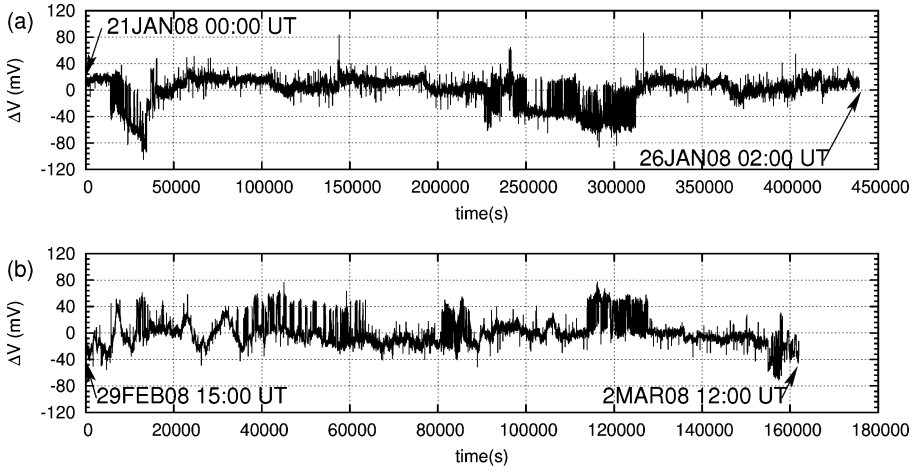

Fig. 3. The most recent long duration SES activities recorded at PIR: (a) Jan. 21–26, 2008, (b) Feb. 29–Mar. 2, 2008.

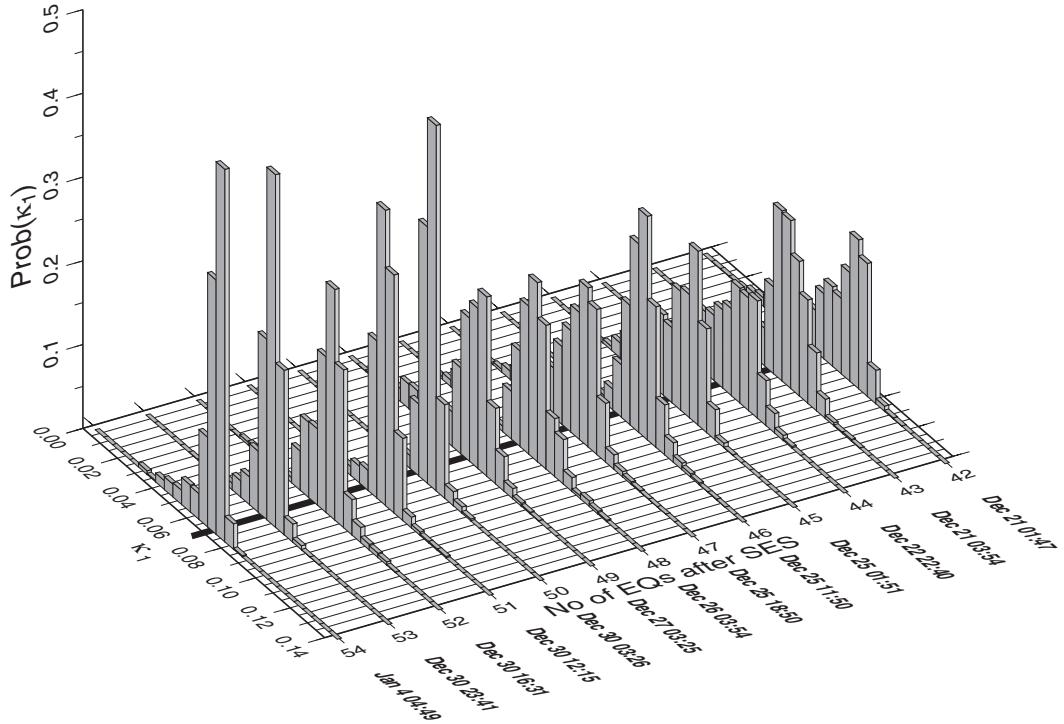

Fig. 4. Study of the Prob(κ_1) for the seismicity ($M_{thres} = 3.2$) that occurred within the area $N_{37.6}^{38.6} E_{20.0}^{23.3}$ after the SES activity at PAT on Nov. 7, 2007.

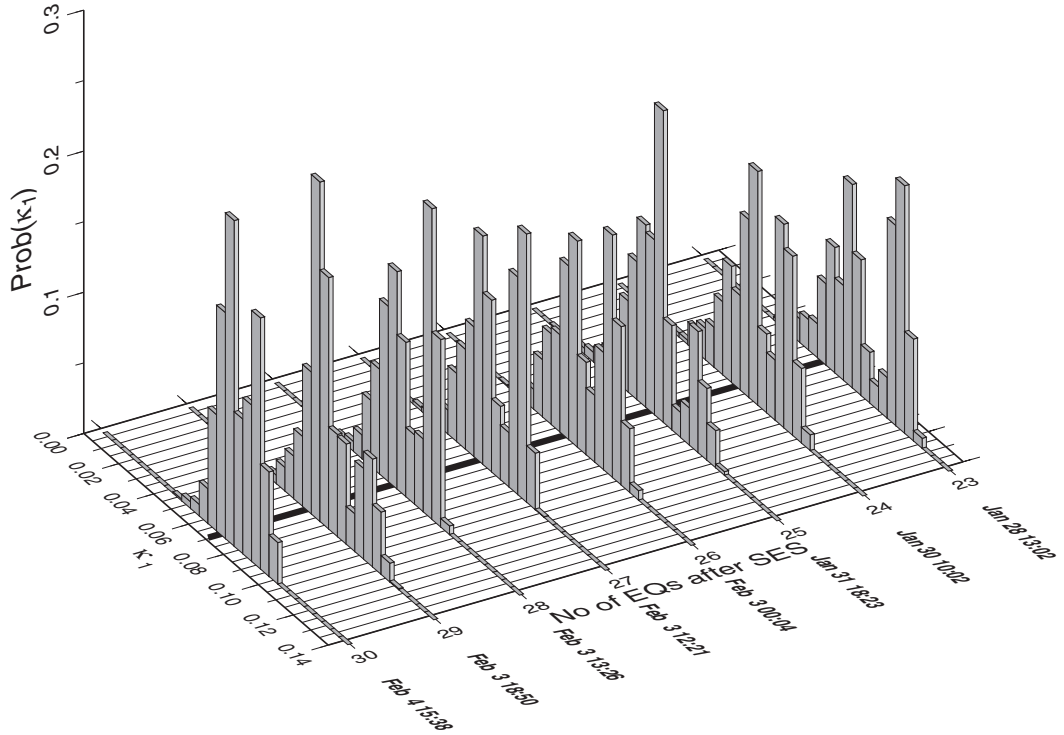

Fig. 5. The same as Fig. 4, but for the SES activity at PAT on Jan. 10, 2008.

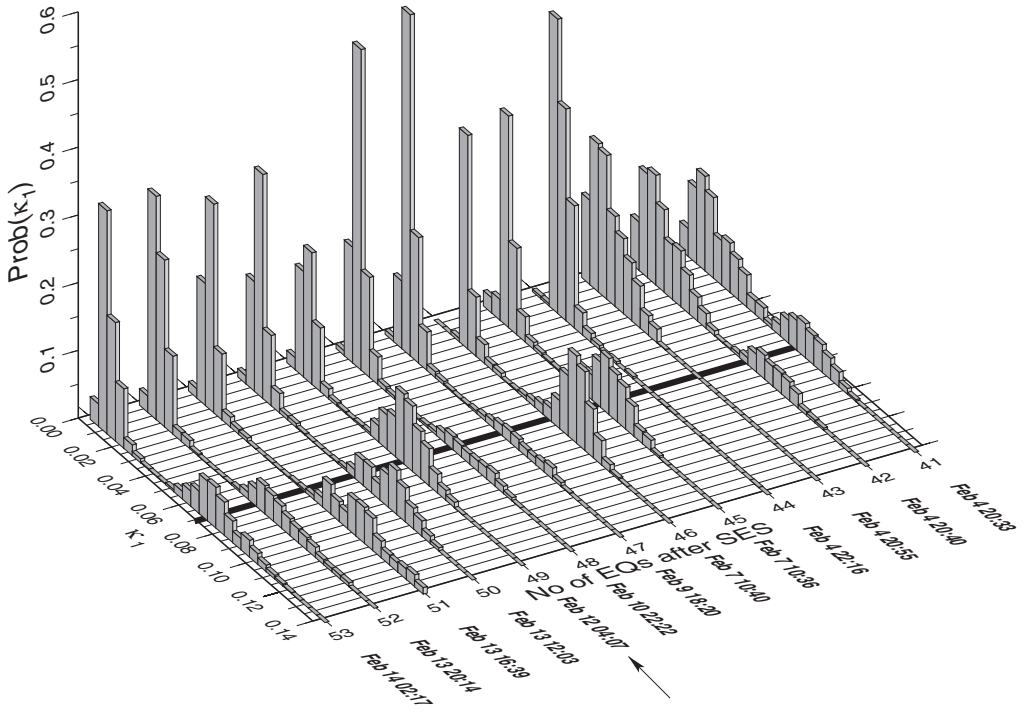

Fig. 6. The same as Fig. 4, but for the area $N_{36.0}^{38.6}E_{20.0}^{22.5}$ after the SES activity at PIR on Jan. 14, 2008.

3.3 The case of the SES activities at PIR on Jan. 14 and Jan. 21–26, 2008. When the first SES activity was recorded on Jan. 14, 2008 at PIR (Fig. 2(c)), the study of the seismicity was immediately started in the area A, i.e., PIR selectivity map area $\mathrm{N}_{36.0}^{38.6}\mathrm{E}_{20.0}^{22.5}$ as indicated in Ref. 40). Almost one week later, a long duration SES activity of the same polarity and amplitude was recorded also at PIR (Fig. 3(a)). The results of the computation are depicted in Fig. 6 ($\mathrm{M_{thres}} = 3.2$), which reveals that Prob(κ_1) also exhibits a clear bimodal feature, one mode of which maximizes at $\kappa_1 \approx 0.070$ upon the occurrence of a small event at 04:07 UT on Feb. 12, 2008 (shown by an arrow). Almost two days later, i.e., at 10:09 UT on Feb. 14, 2008, a major EQ of magnitude 6.7 occurred at 36.5°N 21.8°E, i.e., inside the area A shown by the rectangle with broken lines in Fig. 8. This EQ—according to USGS catalogue (which reported Mw6.9)—is the strongest EQ that occurred in Greek area during the last twenty five years. A few hours later, i.e., at 12:08 UT, a M6.6 EQ, which could have been an aftershock, occurred at 36.2°N 21.8°E. The bimodal feature in Fig. 6 might also be related to the occurrence of the two large EQs, but the mechanism is unclear. In addition, because there were two major SES activities in the month of January, i.e., before the two major Feb. 14 EQs, there is a possibility that the occurrence of these two large EQs might have been related with the appearance of these two SES activities. In fact, it might even be more proper to regard the two SES activities and two large EQs, occurring in a short span of time and space, as representing a single episode of SES activity and correlated seismic activity.

3.4 The case of the SES activity at PAT on Feb. 9, 2008. For this SES activity (Fig. 2(d)), the up to date results (i.e., until early in the morning on Mar. 19, 2008) of the study of the seismicity in the area[41] A: $\mathrm{N}_{37.5}^{38.6}\mathrm{E}_{20.0}^{23.3}$ indicate that Prob(κ_1) has not exhibited a clear maximum at $\kappa_1 \approx 0.070$ yet (see Fig. 7). It can be observed that the distribution also has been bimodal. This investigation is still in progress.

3.5 The case of the SES activity at PIR during the period Feb. 29 to Mar. 2, 2008. This was another long duration SES activity (see Fig. 3(b)). The investigation of the subsequent seismicity is underway. This time the investigation is conducted at first[41] in the area $\mathrm{N}_{37.0}^{38.6}\mathrm{E}_{20.0}^{22.0}$, which is

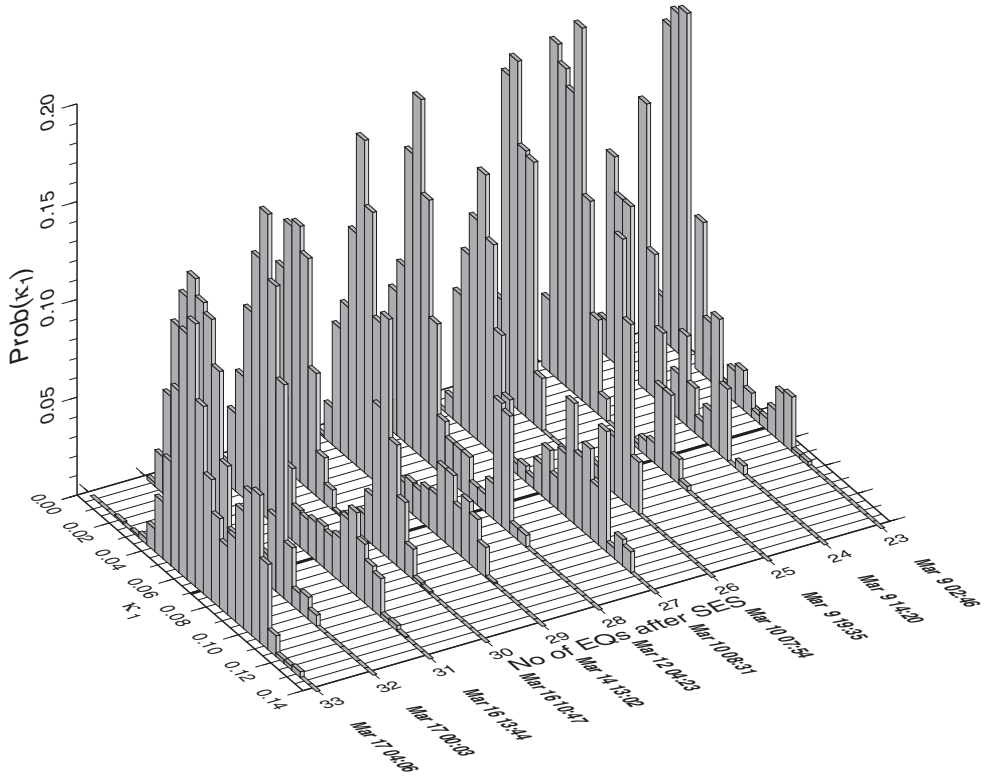

Fig. 7. The same as Fig. 4, but for the area $N_{37.5}^{38.6}E_{20.0}^{23.3}$ after the SES activity at PAT on Feb. 9, 2008 (until Mar. 19, 2008, see the text).

smaller than the known PIR selectivity area $N_{36.0}^{38.6}E_{20.0}^{22.5}$. This was in an attempt to avoid as much as possible the influence of aftershocks of the Mw6.9 EQ at 36.5°N 21.8°E on Feb. 14, 2008. This policy was considered justified, based on the notion stated in the end of Section 2 that a criticality approach would take place in proper subareas simultaneously. At the same time, an attempt is also made to extend the area A to include the shaded area along the Hellenic Arc as shown in Fig. 8. This extension is based on the recent pieces of information for PIR sensitivity map, including the occurrences of the aforementioned Mw6.9 EQ on Feb. 14, 2008 and the Mw6.7 EQ at 36.3°N 23.2°E on Jan. 8, 2006 following the long duration SES activity on Sept. 17, 2005 at PIR.[42] In the study for the extended PIR selectivity map area (Fig. 8), we raised the magnitude threshold to $M_{thres} = 3.9$, 4.0 and 4.1, because the extended area along the Hellenic Arc is highly seismic and there were too many (more than half a thousand) events to handle for $M_{thres} = 3.2$.

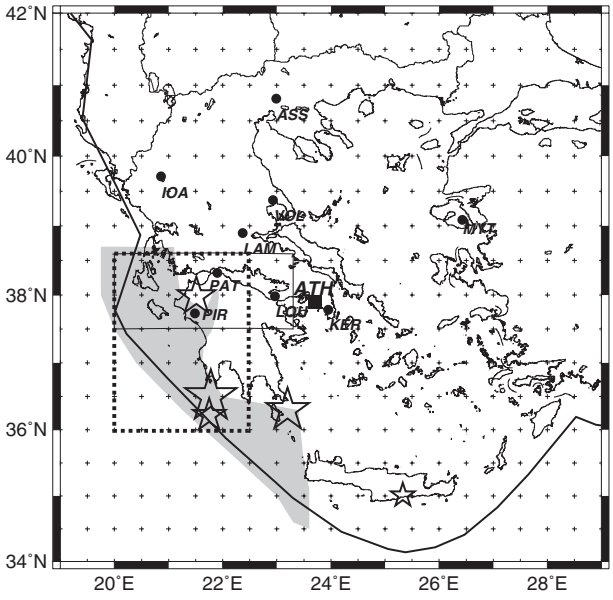

Fig. 8. The shaded area shows the up to date addition to the PIR selectivity map. Solid dots show the measuring stations, while the asterisks denote the epicenters of the EQs discussed in the text that were preceded by SES recorded at PIR. The rectangle with solid lines corresponds to the area A: $N_{37.5}^{38.6}E_{20.0}^{23.3}$ while the one with broken lines to $N_{36.0}^{38.6}E_{20.0}^{22.5}$ (see text).

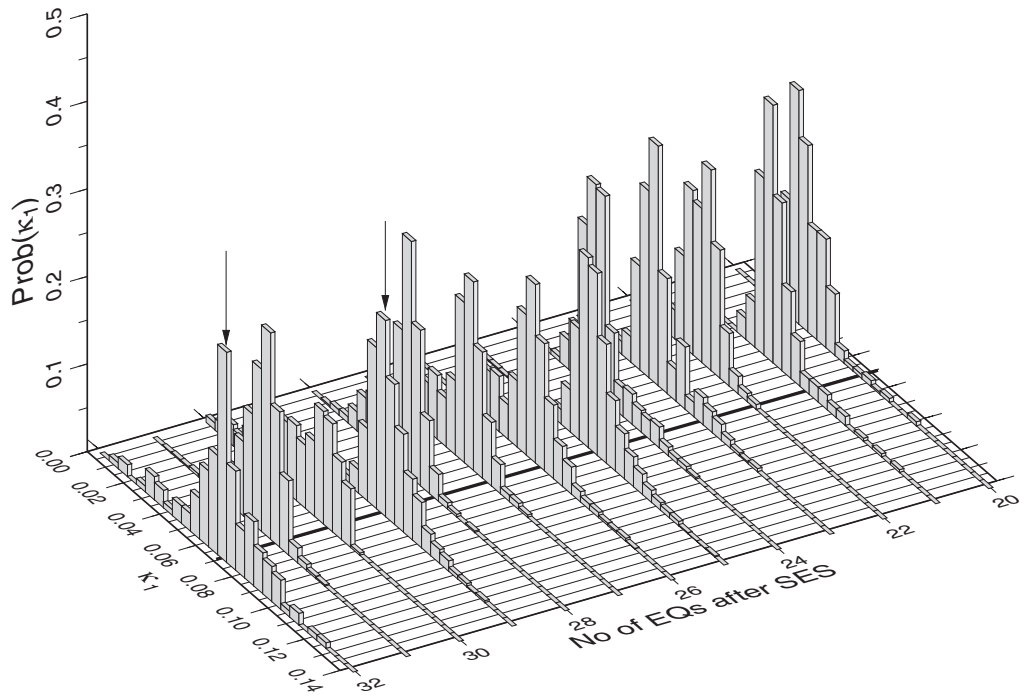

Fig. A-1. Prob(κ_1) versus κ_1 of the seismicity, for $M_{thres} = 3.9$, (subsequent to the long duration SES activity recorded at PIR during Feb. 29 to Mar. 2, 2008) within the shaded area shown in Fig. 8. The two arrows mark the maxima at $\kappa_1 \approx 0.070$ that occurred on May 8, 2008 (i.e., on the occurrence of the 29th event after the SES) and on May 27, 2008 (i.e., on the occurrence of the 32nd event after the SES). The first maximum has been followed by the 5.6 EQ on May 10, 2008, as described in the Appendix.

4. Conclusion

Upon the recording of an SES activity, one can estimate an area within which the impending main shock is expected to occur based on the selectivity map of the station concerned. Following the subsequent seismicity, the probability density function of κ_1 is obtained, which maximizes at $\kappa_1 \approx 0.070$ usually around a few days before the occurrence of the main shock. This indicates the possibility of making the prediction of the occurrence time of major EQs with time window of the order of a week or less.

Appendix

After the first submission (Mar. 21, 2008) of the present paper, the ongoing investigation (Subsection 3.5) of seismicity (for $M_{thres} = 3.2$) in the area $N_{37.0}^{38.6}E_{20.0}^{22.0}$, after the SES activity of Feb. 29 to Mar. 2, 2008 recorded at PIR (Fig. 3(b)), showed maximizations of Prob(κ_1) at $\kappa_1 \approx 0.070$ on Mar. 25 and May 8. The former was followed by a Mar. 28 Ms(ATH) = 5.7 EQ (PDE of USGS reported Mw = 5.6), at 35.0°N 25.3°E (see added star in Fig. 8) approximately 150 km to the east of the PIR selectivity map shown by the shaded area in Fig. 8 and the latter was followed by a May 10 Ms(ATH) = 5.6 EQ at 36.4°N 22.3°E. However, these EQs were considered to be too small for the main shock of the observed SES activity (Fig. 3(b)), because its amplitude was comparable to those of the earlier SES activities also recorded at PIR, including the one depicted in Fig. 3(a) and the one on Sept. 17, 2005,[42] both of which were followed by magnitude 6∼7 class EQs. Therefore, the study of the seismicity in the extended PIR selectivity map area (Fig. 8) still continues to see if a more pronounced peak of Prob(κ_1) at $\kappa_1 \approx 0.070$ will eventually occur in the near future.

Note added[43] *on May 29, 2008.* Upon the occurrence of a Ms(ATH) = 5.1 EQ at 35.5°N 22.4°E at 23:26 UT on May 27 (practically May 28), 2008, Prob(κ_1) exhibits a pronounced maximum at $\kappa_1 \approx 0.070$ marked by an arrow in Fig. A-1 drawn for $M_{thres} = 3.9$ (An additional arrow marks an earlier

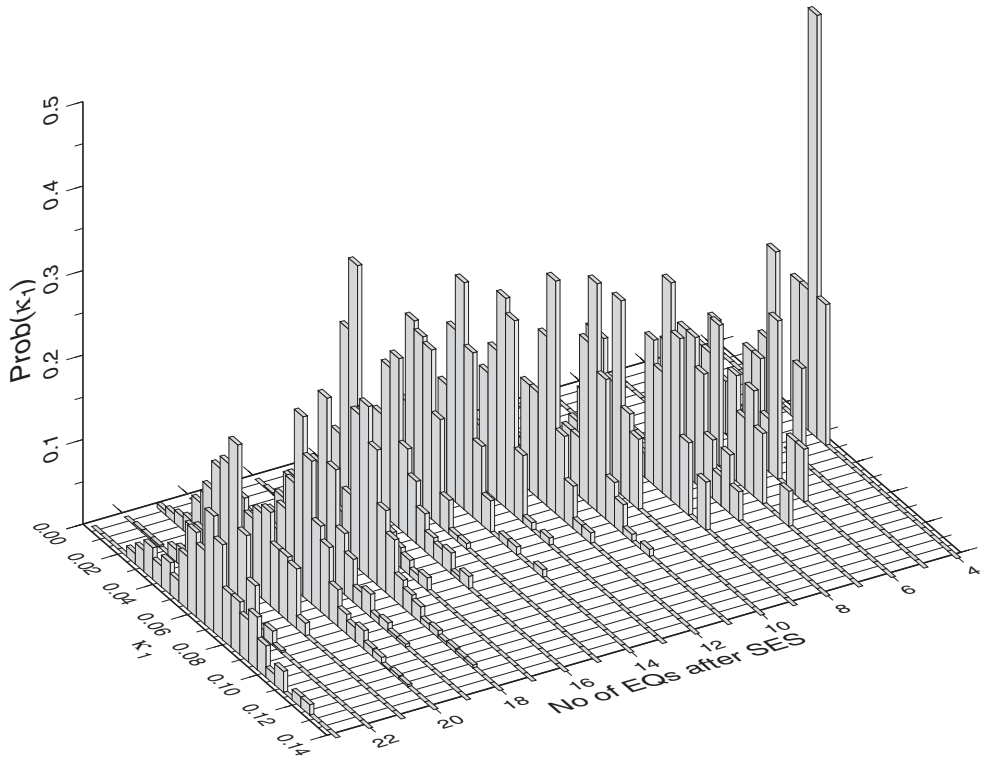

Fig. A-2. The same as Fig. A-1, but for $M_{thres} = 4.0$. The last histogram corresponds to the 5.1 event on May 27, 2008 and exhibits a maximum at $\kappa_1 \approx 0.070$.

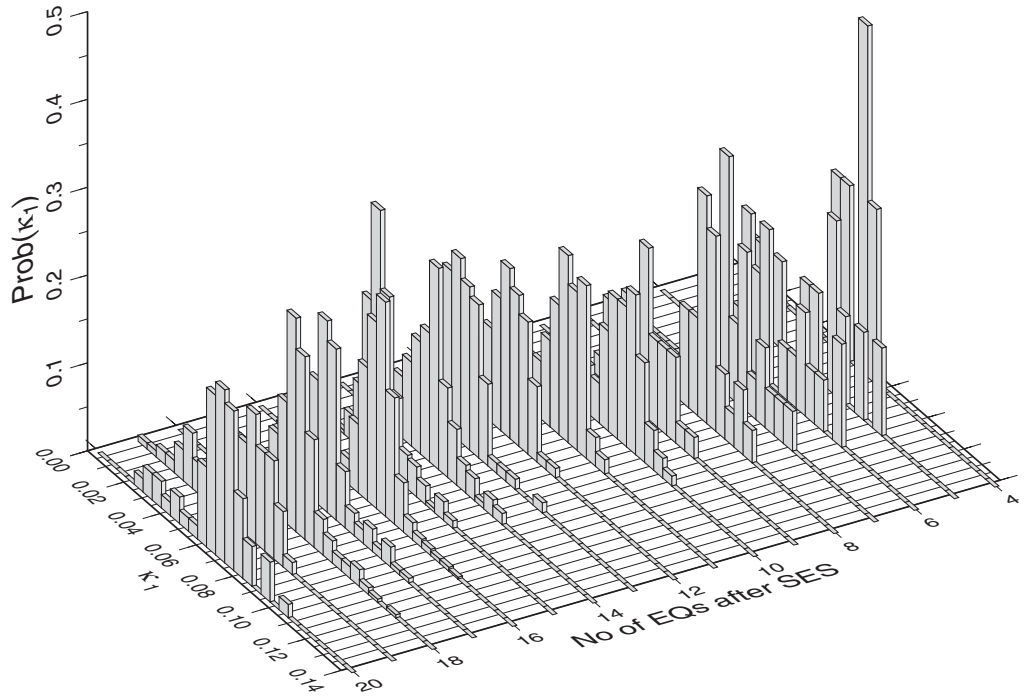

Fig. A-3. The same as Fig. A-1, but for $M_{thres} = 4.1$. The last histogram corresponds to the 5.1 event on May 27, 2008 and exhibits a maximum at $\kappa_1 \approx 0.070$.

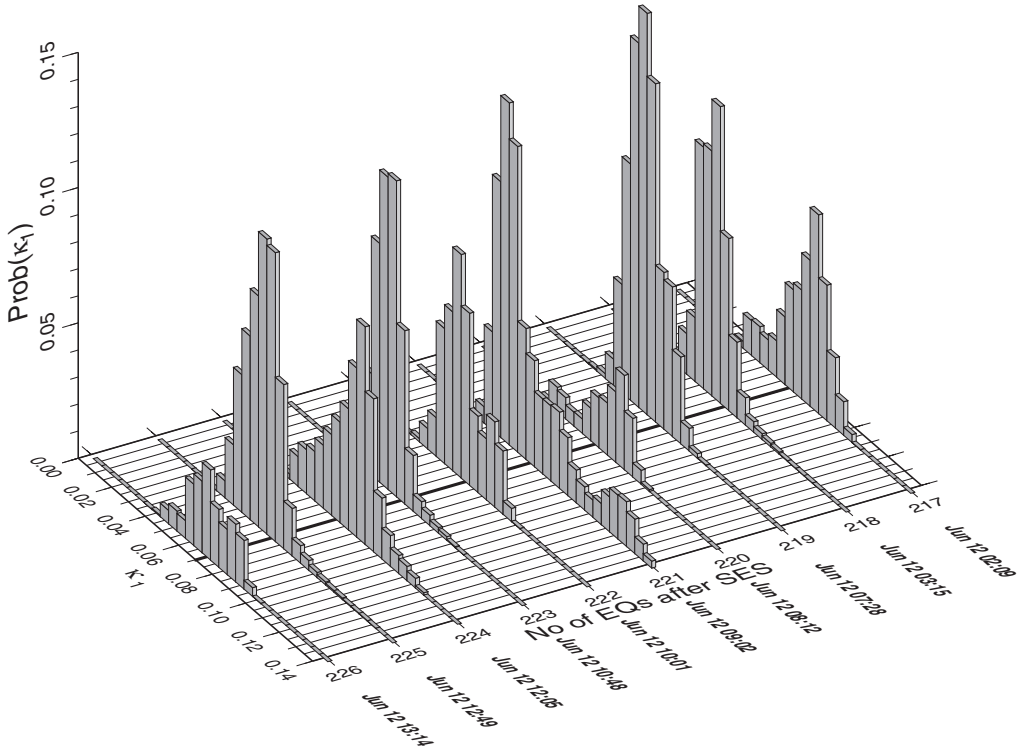

Fig. A-4. Prob(κ_1) versus κ_1 of the seismicity (for $M_{thres} = 3.2$) that occurred within the area $N_{37.5}^{38.6}E_{20.0}^{23.3}$ after the SES activity at PAT on Feb. 9, 2008. The last histogram corresponds to the 3.3 event at 13:14 UT on June 12, 2008 and exhibits a maximun at $\kappa_1 = 0.070$.

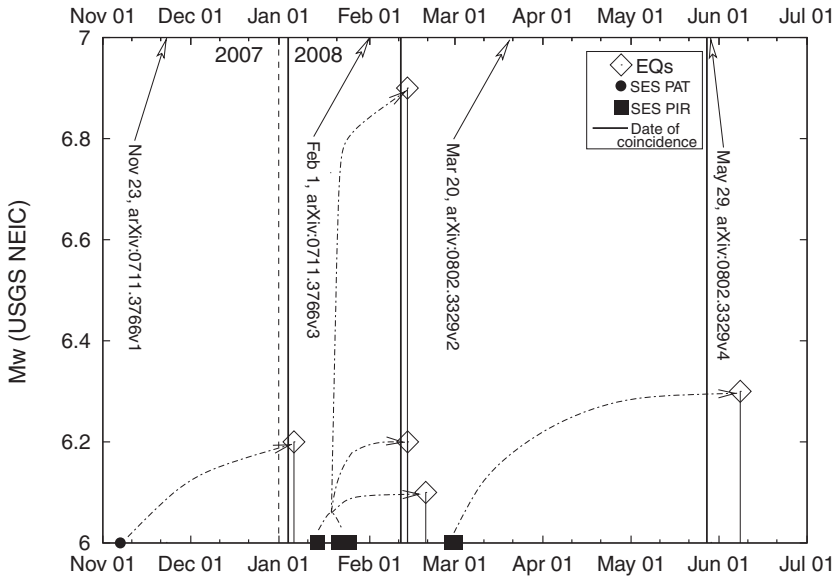

Fig. A-5. Correlations between EQs, associated SES activities, dates of coincidence and arXiv papers. All the EQs with Mw $\geq$ 6.0 that occurred in the Greek area during the period: Nov. 1, 2007–July 1, 2008 are shown by diamonds. The associated SES activities are placed on the horizontal axis. Coincidence dates are shown by vertical solid lines. Slanted upward arrows point at the dates of the arXiv papers reporting SES activity appearance (arrows on Nov. 23, 2007; Feb. 1 and Mar. 20, 2008) and coincidence (arrow on May 29, 2008). The Mw = 6.1 EQ on Feb. 20, not mentioned in the text, is an aftershock of the 6.9Mw event on Feb. 14, 2008. It can be seen that the main shocks occur with very short time-windows after the coincidence, whereas SES and coincidence are not necessarily too close in time.

maximum on May 8, 2008 that preceded the aforementioned Ms(ATH) = 5.6 EQ on May 10, 2008, see the Appendix). Similar maximum at $\kappa_1 \approx 0.070$ appears simultaneously for $M_{thres} = 4.0$ and $M_{thres} = 4.1$ as shown by Figs. A-2 and A-3, respectively.

Note added on June 9, 2008. Actually, at 12:25 UT on June 8, 2008, a magnitude 6.5 (Harvard reported Mw = 6.3) EQ occurred at 38.0°N 21.5°E, i.e., inside the candidate area A (Fig. 8). It caused extensive damage (four people were killed while several hundred houses were seriously damaged). The magnitude expected from the amplitude of the SES activity, as mentioned in the last paragraph of Appendix, was reasonably well supported by the actual EQ.

Note added on June 19, 2008. The up-dated results of the study of the seismicity in the area A: $N_{37.5}^{38.6}E_{20.0}^{23.3}$ (shown by the rectangle with solid lines in Fig. 8), subsequent to the SES activity at PAT on Feb. 9, 2008 (Subsection 3.4), are shown in Fig. A-4. In this figure, Prob(κ_1) exhibits a maximum at $\kappa_1 = 0.070$ at 13:14 UT on June 12, 2008. This maximum was followed by a M5.6 EQ at 01:58 UT on June 18, 2008 at 37.7°N 22.8°E (almost 90 km ESE of PAT) lying inside the area A.

For the sake of reader's convenience, all EQs with Mw $\geq$ 6.0 that occurred in the Greek area during the period Nov. 1, 2007 to July 1, 2008 along with the associated SES activities are summarized in Fig. A-5.

References

1) Varotsos, P. and Alexopoulos, K. (1984) Tectonophysics **110**, 73–98.
2) Varotsos, P. and Alexopoulos, K. (1984) Tectonophysics **110**, 99–125.
3) Varotsos, P., Alexopoulos, K., Nomicos, K. and Lazaridou, M. (1988) Tectonophysics **152**, 193–196.
4) Varotsos, P. and Lazaridou, M. (1991) Tectonophysics **188**, 321–347.
5) Varotsos, P., Alexopoulos, K. and Lazaridou, M. (1993) Tectonophysics **224**, 1–37.
6) Varotsos, P., Sarlis, N. and Lazaridou, M. (1999) Phys. Rev. B **59**, 24–27 (doi: 10.1103/PhysRevB.59.24).
7) Sarlis, N., Lazaridou, M., Kapiris, P. and Varotsos, P. (1999) Geophys. Res. Lett. **26**, 3245–3248.
8) Uyeda, S., Nagao, T., Orihara, Y., Yamaguchi, T. and Takahashi, I. (2000) Proc. Natl. Acad. Sci. USA **97**, 4561–4566.
9) Uyeda, S., Hayakawa, M., Nagao, T., Molchanov, O., Hattori, K., Orihara, Y., Gotoh, K., Akinaga, Y. and Tanaka, H. (2002) Proc. Natl. Acad. Sci. USA **99**, 7352–7355.
10) Flores-Márquez, L., Márquez-Cruz, J., Ramirez-Rojas, A., Gálvez-Coyt, G. and Angulo-Brown, F. (2007) Nat. Hazards Earth Syst. Sci. **7**, 549–556.
11) Varotsos, P. and Alexopoulos, K. (1986) Thermodynamics of Point Defects and Their Relation with Bulk Properties. North Holland, Amsterdam, pp. 137–420.
12) Varotsos, P. (2005) The Physics of Seismic Electric Signals. TERRAPUB, Tokyo, pp. 8–21, 256–304.
13) Varotsos, P.A. (1977) J. Phys. (France) Lettr. **38**, L455–L458.
14) Varotsos, P. and Alexopoulos, K. (1978) Phys. Stat. Solidi A **47**, K133–K136.
15) Lazaridou, M., Varotsos, C., Alexopoulos, K. and Varotsos, P. (1985) J. Phys. C: Solid State **18**, 3891–3895.
16) Bak, P., Christensen, K., Danon, L. and Scanlon, T. (2002) Phys. Rev. Lett. **88**, Art. No. 178501 (doi: 10.1103/PhysRevLett.88.178501).
17) Corral, A. (2004) Phys. Rev. Lett. **92**, Art. No. 108501 (doi: 10.1103/PhysRevLett.92.108501).
18) Baiesi, M. and Paczuski, M. (2004) Phys. Rev. E **69**, Art. No. 066106 (doi: 10.1103/PhysRevE.69.066106).
19) Tanaka, H. K., Varotsos, P. A., Sarlis, N. V. and Skordas, E. S. (2004) Proc. Jpn. Acad., Ser. B **80**, 283–289.
20) Abe, S. and Suzuki, N. (2004) Europhys. Lett. **65**, 581–586.
21) Shebalin, P. (2006) Tectonophysics **424**, 335.
22) Holliday, J.R., Rundle, J.B., Turcotte, D.L., Klein, W., Tiampo, K.F. and Donnellan, A. (2006) Phys. Rev. Lett. **97**, Art. No. 238501 (doi:10.1103/PhysRevLett.97.238501).
23) Tiampo, K.F., Rundle, J.B., Klein, W., Holliday, J., Martins, J.S.S. and Ferguson, C.D. (2007) Phys. Rev. E **75**, Art. No. 066107 (doi:10.1103/PhysRevE.75.066107).
24) Klein, W., Gould, H., Gulbahce, N., Rundle, J.B. and Tiampo, K. (2007) Phys. Rev. E **75**, Art. No. 031114 (doi:10.1103/PhysRevE.75.031114).
25) Sornette, D. (2004) Critical Phenomena in Natural Science. 2nd ed., Springer, Berlin.
26) Varotsos, P., Sarlis, N. and Skordas, E. (2001) Practica of Athens Acad. **76**, 294–321.
27) Varotsos, P.A., Sarlis, N.V. and Skordas, E.S. (2002) Phys. Rev. E **66**, Art. No. 011902 (doi: 10.1103/PhysRevE.66.011902).
28) Varotsos, P.A., Sarlis, N.V., Tanaka, H.K. and Skordas, E.S. (2005) Phys. Rev. E **72**, Art. No. 041103 (doi: 10.1103/PhysRevE.72.041103).
29) Feller, W. (1971) An Introduction to Probability Theory and its Applications. 2nd Vol., John Wiley & Sons, New York, p. 499, 512, 514.
30) Varotsos, P.A., Sarlis, N.V. and Skordas, E.S. (2003) Phys. Rev. E **68**, Art. No. 031106 (doi: 10.1103/PhysRevE.68.031106).
31) Varotsos, P.A., Sarlis, N.V., Tanaka, H.K. and Skordas, E.S. (2005) Phys. Rev. E **71**, Art.

No. 032102 (doi: 10.1103/PhysRevE.71.032102).
32) Varotsos, P.A., Sarlis, N.V., Skordas, E.S. and Lazaridou, M.S. (2004) Phys. Rev. E **70**, Art. No. 011106 (doi: 10.1103/PhysRevE.70.011106).
33) Varotsos, P.A., Sarlis, N.V., Skordas, E.S., Tanaka, H.K. and Lazaridou, M.S. (2006) Phys. Rev. E **73**, Art. No. 031114 (doi: 10.1103/PhysRevE.73.031114).
34) Varotsos, P.A., Sarlis, N.V., Skordas, E.S., Tanaka, H.K. and Lazaridou, M.S. (2006) Phys. Rev. E **74**, Art. No. 021123 (doi: 10.1103/PhysRevE.74.021123).
35) Varotsos, P.A., Sarlis, N.V., Skordas, E.S. and Lazaridou, M.S. (2008) J. Appl. Phys. **103**, Art. No. 014906 (doi: 10.1063/1.2827363).
36) Varotsos, P. and Alexopoulos, K. (1987) Tectonophysics **136**, 335–339.
37) Kondo, S., Uyeda, S. and Nagao, T. (2002) J. Geodynamics **33**, 433.
38) Varotsos, P., Sarlis, N., Skordas, E. and Lazaridou, M. (2006) Tectonophysics **412**, 279–288.
39) Varotsos, P.A., Sarlis, N.V. and Skordas, E.S. (2007) arXiv:0711.3766v1 (November 23, 2007).
40) a) Varotsos, P.A., Sarlis, N.V. and Skordas, E.S. (2008) arXiv:0711.3766v3 (February 1, 2008); b) Uyeda, S. and Kamogawa, M. (2008) Eos 89, No. 39, 23 Sept., 2008.
41) Sarlis, N.V., Skordas, E.S., Lazaridou, M.S. and Varotsos, P.A. (2008) arXiv:0802.3329v1 (February 22, 2008).
42) Varotsos, P.A. (2006) Proc. Jpn. Acad., Ser. B **82**, 86–91.
43) Sarlis, N.V., Skordas, E.S., Lazaridou, M.S. and Varotsos, P.A. (2008) arXiv:0802.3329v4 (May 29, 2008).

(Received Mar. 21, 2008; accepted Sept. 4, 2008)